Coatings for Hypersonic Rockets

Team Members: Selin Cetin, Souhardya Pal, Zachary Vexler

Abstract

The advances made in aerospace over the past century have changed human history irrevocably. The impact of the this industry can be seen in defense and transportation sectors, and space exploration has allowed humans to reach new understandings of physics and the universe. Student clubs have sprung up around aerospace, Northwestern's NUSTARS being one such group, allowing members to explore the foundations of rocketry in a hands-on context. One feat that very few student groups have accomplished is a rocket launch that reaches space. To achieve this, we believe the use of a specially-designed coating applied to the nose cone of the rocket will be effective. The rocket will need to travel at hypersonic speeds to reach space, which presents a number of challenges, the primary one being extremely high temperatures. In this paper, a coating which allows a student-designed rocket to withstand hypersonic flight conditions and reach space is designed.

Introduction

Space exploration has piqued human interest since the mid-twentieth century. Initially a case of wanting to discover previously unknown realms, aerospace exploration soon translated to a wide array of benefits for humanity. Satellites sent from Earth have allowed scientists to not only learn more about the planets around us, but have also provided crucial data which have aided developments in weather reporting, global positioning and telecommunications [1]. The aerospace industry is one the fastest-growing sectors today, with further investments being made to achieve targets such as human access to Mars.

For a rocket to reach space, it must be able to break through the barrier of the Earth's atmosphere, which will require reaching very high speeds. In order to do this, the rocket must be designed to include properties such as low area density, high temperature resistance, and a low drag coefficient. A key feature of the rocket is the nose cone, which is the nozzle-like structure which acts as the head of the rocket. Not only must this part have a shape which translates to suitable aerodynamic performance, but it must also be able to withstand very high temperatures and drag forces during flight. To accomplish this, a coating for the nose cone is used to provide the rocket a significant performance boost. Coatings act to provide a layer of protection for the exoskeleton of the rocket from the surrounding environment, and must be chemically compatible with the substrate that they are being applied on.

For our Materials Design project, we are designing a coating for the nose cone of a student-built hypersonic rocket. The rocket will be designed by NUSTARS, which is a student-run group operating in Northwestern University aiming to explore and teach the field of rocketry to students on campus. Our process of designing this coating required us to decide on the most significant properties and determine a material that possessed these properties and could also be viably manufactured by the team. Furthermore, COMSOL Multiphysics [2] finite element modeling allowed us to investigate the feasibility of our designs. We then identified the optimal structural elements for our material based on the desired properties. Key aspects in designing the coating included ensuring that it was cost-effective and that its synthesis could be conducted in a university lab. We predict that our coating will allow the rocket to survive hypersonic speeds and reach space, which is the final target of this project.

Project Nose Cone Design

The nose cone optimized in this design project has three primary components. A visual example can be seen in Figure 1 [3]. The tip of the nose cone is Inconel, which is a high temperature resistant metal that is

frequently used for this purpose. A different material is chosen for the tip because the tip of the nose cone and the body region of the nose cone experience significantly different conditions. The tip is a stagnation point for fluid flow, which means that heat and force are concentrated at this point and are experienced at far higher magnitudes than in the body region. Thus, it is justifiable to use a material that can withstand these conditions at this point, even though it adds a significant amount of weight since it is a dense metal. The body region, indicated by the red dot, consists of two components: a fiberglass cone inside and the coating that we have designed outside. Fiberglass is a material commonly used by NUSTARS for their nose cones. In this application, it is a better choice than carbon fiber, which is another common nose cone material, since fiberglass is radio frequency (RF) transparent. This is desirable in the event that electronics are housed in the nose cone. Our focus in this project is on a coating surrounding and protecting this fiberglass.

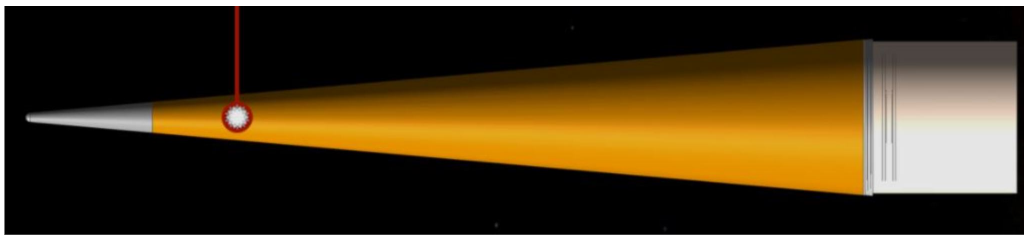

Figure 1: Nose cone

System Design Chart

A systems design chart is used to identify the relationships between the processing of a material, its structure, properties, and performance. Before explaining our systems design chart, shown in Figure 2, the general design of our coating must be established. During our design process, we decided to use a dual-layer coating. The inner coating is a foam, and the outer coating is a paint. The rationale behind these decisions will be expanded upon in subsequent sections, but the basic design is requisite to fully understand the design chart. The focal elements of our design project and their relationships are highlighted in black on the chart, and explained in greater detail below.

Performance → Properties The most crucial performance metric targeted in our design is that of high temperature resistance. This is influenced by thermal properties such as thermal diffusivity or ablation capabilities. Mechanical stability is another important performance metric, as the coating must be able to withstand the forces experienced during flight, as well as general stresses that would occur during rocket construction and testing. This metric is controlled by mechanical properties such as fracture toughness and yield strength. Since we are working with a dual-layer coating that will additionally be adhered to a fiberglass substrate, properties relating to interlayer compatibility must be considered as well. These properties include the similarity of thermal expansion coefficients and the strength of bonding. The last two performance metrics we optimized our design for are those dependent on physical properties. The coating must have a low drag coefficient so it does not significantly reduce the speed of the rocket during flight. Additionally, it must be lightweight, to best optimize the speed and flight stability of the rocket.

Properties → Structure Thermal properties, mechanical properties, and physical properties are all heavily influenced by the structure of the foam used. These structural elements include the porosity, the pore size, and the type of foam used, i.e. open-cell or closed-cell. Physical properties are additionally affected by the smoothness of the surface. Properties surrounding interlayer compatibility are primarily determined by the molecular structure.

Structure → Processing Foam structure is largely determined by conditions during deposition, such as the pH level, and conditions directly after deposition, such as the dry time and temperature [4]. The smoothness of the coating surface is clearly affected by surface finishing done after processing. Molecular structure is dependent on the components used during the coating deposition process, as well as the concentrations in which they are used.

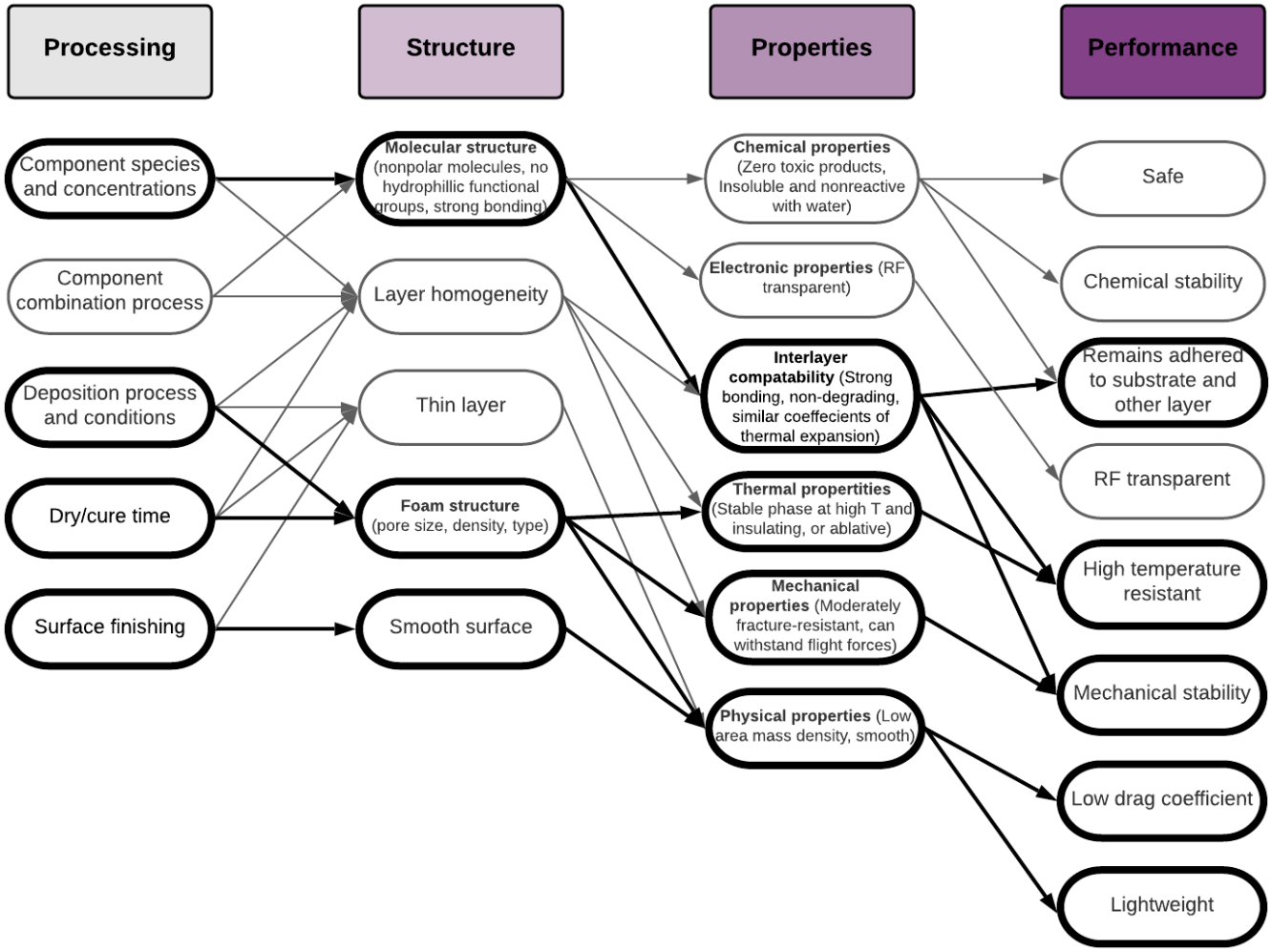

Figure 2: System design chart

Materials Selection

In order to utilize the CES Materials Selector to determine an appropriate coating for our rocket, we had to make some preliminary decisions. We could use either an ablative coating or a coating that could withstand high temperatures without damage. Since CES Materials Selector does not list any materials properties relating to their ablative capabilities, we decided to limit our search to materials that could withstand high temperatures. After performing preliminary COMSOL simulations, we determined that implementing a dual-layer coating would allow us to better meet our performance metrics. Initially, we had investigated a grouping of coatings that are now categorized as options for the outer coatings. While these coatings are still suitable for a thin outer layer, they would need to be manufactured at unreasonable thicknesses to provide the necessary amount of insulation if used as the sole nose cone coating.

Thus, the materials selection process is divided into two stages: one for the outer coating and one for the inner coating. For the outer coating, we needed some conception of the deposition process planned to be used. Processes that NUSTARS could conceivably perform themselves were favored, as the club aims to be as hands-on as possible. Paint is an easy method of deposition that requires very little specialized knowledge or equipment. Chemical vapor deposition (CVD) is an alternate option to paint, as it is a technique commonly used for the application of high temperature resistant coatings. It can be used to coat parts with non-standard geometries, which is necessary given that our nose cone will be curved. However, it is quite complicated and would need to be outsourced [5]. All of the materials selected as options for the outer coating can be deposited via one of these methods. For the inner coating, we did not have to identify a processing method ahead of time; sol-gel arose as the best option after the materials selection process. This process also does not require expensive and specialized equipment, meaning NUSTARS could plausibly do it in-house.

General Selection Procedure The first materials properties that we considered were maximum service temperature and yield strength. The maximum service temperature must be above 1200 °C (1473 K), which is non-negotiable given that this is the temperature expected at Mach 5. We used this for both the inner and outer layers. We were seeking a material moderately resistant to fracture in order to withstand general handling and machining forces. It was more important to us that the outer coating was strong than the inner coating, so we had different maximization thresholds for the yield strength of these two layers. We then added a limit stage to ensure all the materials would react well with water, i.e. be insoluble and inert. We then plotted thermal diffusivity against density to make our final materials selections. Thermal diffusivity is the rate at which heat disperses through a material, and it is given by the equation $\alpha = \frac{k}{\rho C_p}$, where k is thermal conductivity, ρ is density, and C_p is specific heat capacity. We were seeking materials with low thermal diffusivity to protect the nose cone from the outside temperatures, and low density to create a lightweight nose cone. Additionally, we preferentially selected materials that were made of the same base material for the inner and outer layers for ease of processing and to eliminate compatibility concerns. The materials selected for the inner and outer coatings differ, so they are discussed individually below.

Outer Layer As part of the selection process, we ensured that all coatings selected could be deposited via CVD, sol-gel, or paint. Some of the top candidates are labeled in the materials selection chart in Figure 3. Vapor deposited carbon is very lightweight and has low thermal diffusivity, thus making it an optimal outer coating in terms of properties. However, it can only be deposited by CVD, which is the least accessible method. Regardless, the team decided to investigate it based on its superior properties. Alumina and zirconia are the other two materials selected as options for the outer coating. Both of these are available in paint form, which is optimal for manufacturing because of its ease of use. Additionally, both of these have foam counterparts which are discussed in the Inner Layer section. Alumina has relatively high thermal diffusivity but its foam counterpart has superior strength properties. Zirconia has extremely low thermal diffusivity, but it is more dense than the other options.

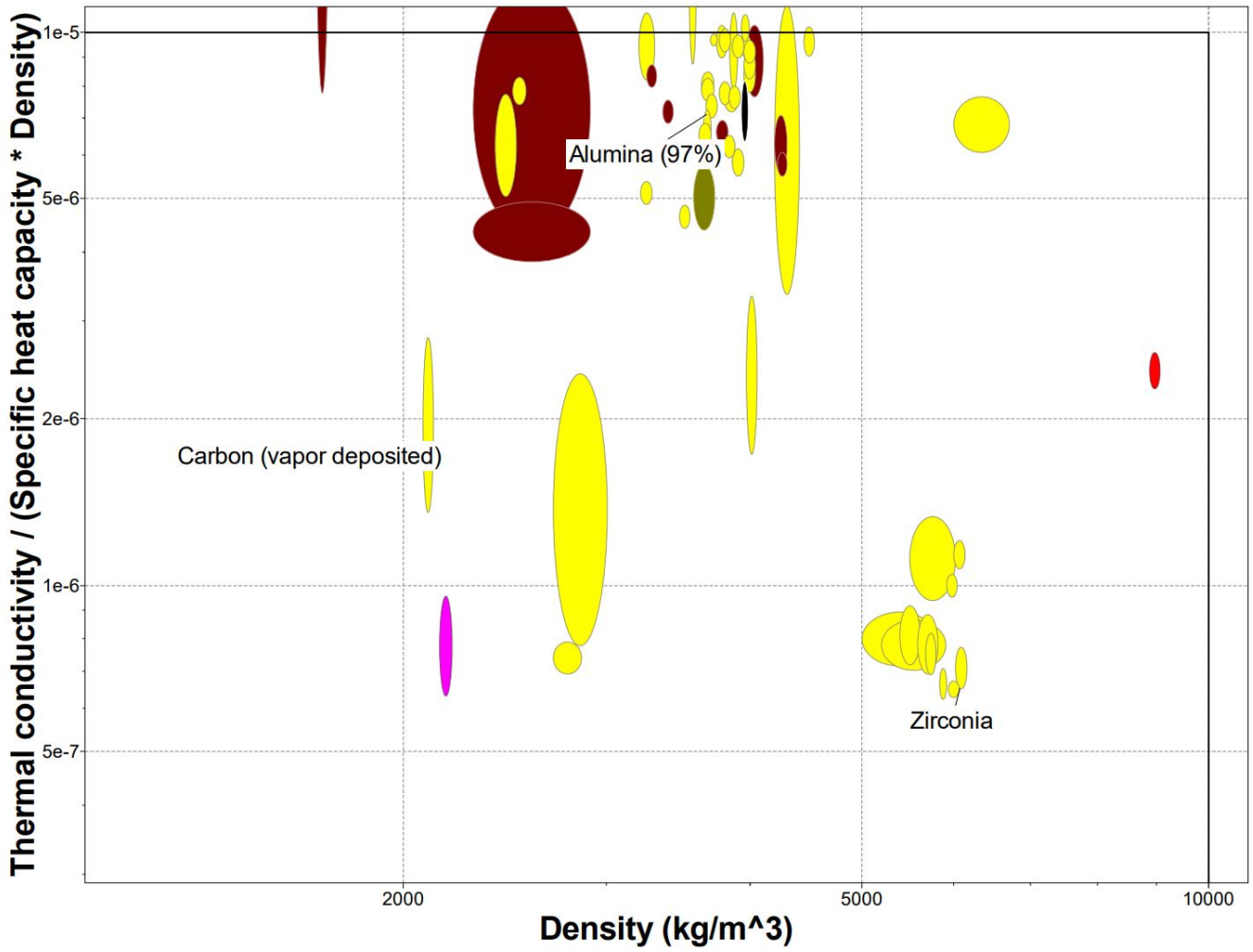

Figure 3: Materials selection chart - Outer layer

Inner Layer As mentioned in the General Selection Procedure section, we preferentially selected materials for the inner layer that had a corresponding candidate for the outer layer made of the same components. This became more important once we realized all of the inner layer candidates were foams. The outer layer would then fill the surface layer of pores and create a smooth surface. Since the outer coating is incorporated into the structure of the inner layer, the compatibility concern of the similarity between the coefficients of thermal expansion becomes particularly pressing. If the outer layer has a larger coefficient of thermal expansion than the inner layer, it will expand more than the inner layer and thus could cause structural damage to the inner layer. The two candidates selected for this inner layer are alumina foam and zirconia foam. Each of these foams possess different desirable qualities. The zirconia foam has a lower thermal diffusivity than the alumina foam, as shown in Figure 4 (the inverse thermal diffusivity is plotted on the y-axis, which differs from Figure 3, where thermal diffusivity is plotted). However, the alumina foam has a higher yield strength than the zirconia foam as shown in Figure 5. Both foams can be manufactured using sol-gel, meaning NUSTARS could opt to create custom-molded foams for the nose cone [6] [7].

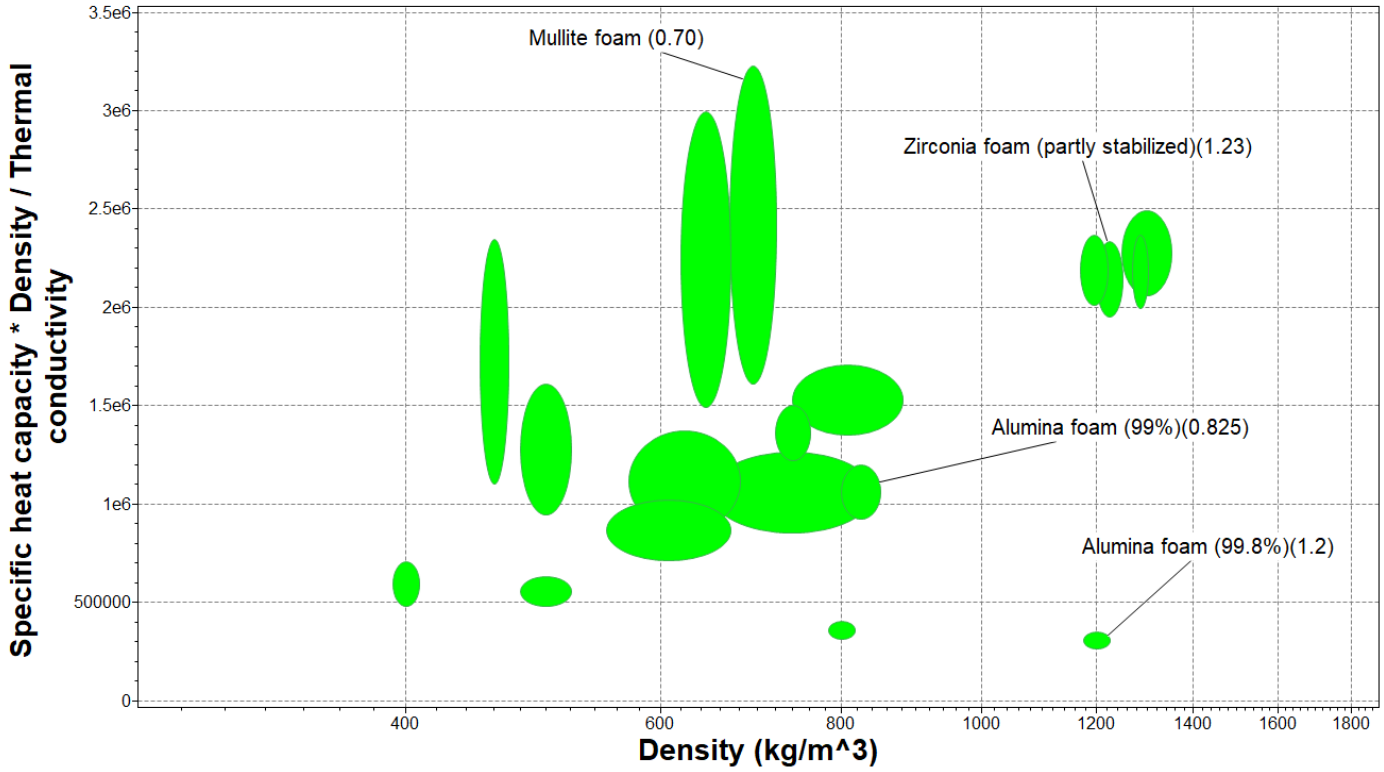

Figure 4: Materials selection chart - Inner layer: Thermal

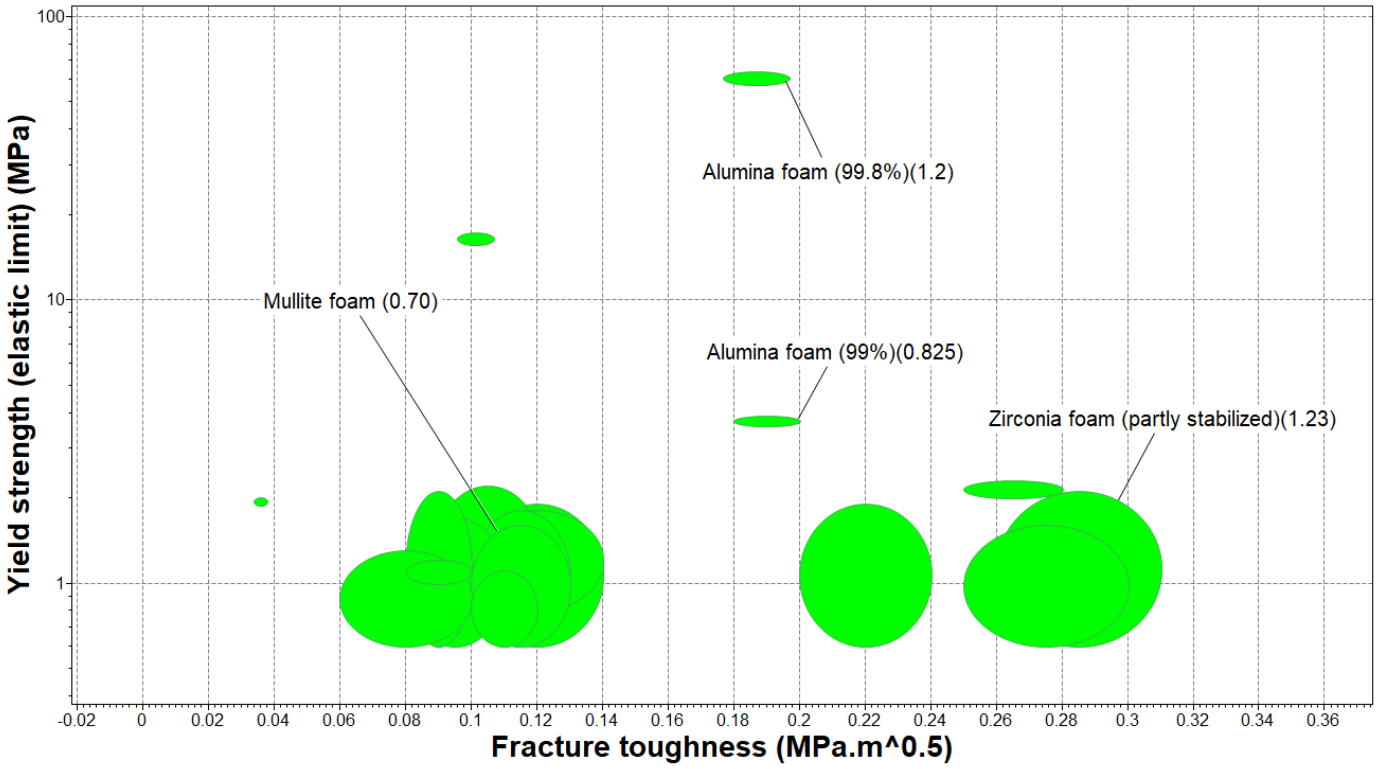

Figure 5: Materials selection chart - Inner layer: Mechanical

Design Strategy

In order to make the final materials selection, we determined that we needed to model the top material candidates. This project revolves around optimizing a material for an extremely specific use-case, so evaluating performance under the conditions of said use-case is a necessity. It must be practical to manufacture a nose cone with the coating thickness needed to protect the substrate; if the thickness of the coating comprises an excessively large portion of the nose cone volume, then it is not a realistic option. We selected zirconia foam with a density of 1.23 $\frac{g}{cm^3}$, alumina foam with densities of 0.825 $\frac{g}{cm^3}$ and 1.2 $\frac{g}{cm^3}$, and vapor deposited carbon as materials to proceed with for modeling.

We had two primary goals that we hoped to accomplish through simulations; the first dealt with the crux of our project, which is the thermal behavior of the nose cone. This goal was to optimize the coating thickness for insulation. So, we needed to determine what coating thickness was necessary to prevent the fiberglass substrate from degradation. This temperature that the substrate could not exceed was designated to be 275 °C. While the maximum service temperature of fiberglass is 112 - 128 °C, the substrate will be experiencing high temperatures for a very short time increment [8]. Because of this short time increment, it is likely that a higher substrate temperature can be withstood. We researched the fiberglass nose cones that NUSTARS typically purchases and found that the degradation temperature listed was 275 °C [9]. To determine this coating thickness, we performed COMSOL simulations of heat transfer throughout the course of the rocket's flight. The first step needed to do this was to determine the temperature profile on the surface of the nose cone for the duration of the flight. This is not a trivial task; to model this, we would need to create a complex CFD simulation. Given the time constraints and our lack of experience with fluids simulations, this was not feasible. The details of how we selected the temperature profile are described in the Temperature Profile section. Once this was done, we were able to model heat diffusion in the coating layer. This was performed in COMSOL by exposing a nose cone entirely composed of the coating material to the temperature profile. From this, we determined the minimum coating thickness necessary to protect the substrate material.

Our second goal for modeling was to test the proposed coating thickness for strength. The nose cone must be able to withstand pressures experienced during flight, the greatest of which we determined to be 0.25 MPa. To find this value, we used a hypersonic rocket simulation software to determine a pressure profile for the duration of the flight and identify the maximum value. We then modeled this maximum pressure value at the nose cone tip in COMSOL and analyzed the behavior of the coated body region. This was necessary to ensure the coating options had sufficiently high strength and would not deform or fracture.

Finally, we investigated the sol-gel technique selected for coating creation. It is through this sol-gel processing that we optimized the structure of our material to best align with our performance metrics.

Temperature Profile

This section discusses the rationale behind the temperature profile used in our simulations. We initially conducted a literature review to determine if there was an existing temperature profile for a similar flight that we could re-purpose for our project. We did not find anything suitable, so we turned to theoretical equations instead, and used the temperature profiles found in literature as validation resources. We used Equation 1, which yields stagnation temperature as a function of Mach number, to create our temperature profile [10]. The Mach number and altitude at each selected time were graphically approximated from the Traveler IV whitepaper [11]. With the ambient temperatures at each altitude [12], the external temperature was found with the stagnation temperature equation. Stagnation temperature is the temperature that would be experienced if the moving flow of a fluid was isentropically halted. This is also the temperature that occurs at the stagnation point of a moving body in a fluid. In this case, the stagnation point is the tip of the nose cone. This temperature will be much higher than the temperature experienced by the majority of the nose cone, so it is a significant overestimate to use it for the entirety of the nose cone. Since the tip of the nose cone is made of Inconel and the remaining body region is made of the material selected in this paper, it is

likely that the body regions of the nose cone that we are concerned with will never experience the maximum stagnation temperature predicted. By using the temperature as the skin temperature of the entire nose cone, this simply ensures that there is a built-in safety factor in our simulations.

$$T_t = T(1 + \frac{\gamma - 1}{2} M^2) \tag{1}$$

As an alternative option, a hypersonic simulation software, HyperCFD, was used to compute a temperature profile for the body region of the nose cone. We calculated significantly lower temperatures for the body than predicted with the stagnation temperature calculations, however, upon comparing these results to empirical data, we concluded that the predicted temperatures were too low to comfortably use. The empirical data was taken from a rocket flight that reached Mach 10.4. This rocket had a blunted nose cone like our design, and the overall geometry was reasonably similar to ours [13]. Thermocouples on the surface of the rocket measured skin temperature for the duration of the flight. Although this flight trajectory did not align closely enough with our flight trajectory for us to directly use the data, we did determine that the HyperCFD skin temperatures were likely below what would be experienced by the rocket. So, faced with the options of using an overestimating temperature profile that fit our flight data exactly, an empirical temperature profile that only would've sufficed for one region of the flight, or an underestimating temperature profile that fit our flight data exactly, we opted to use the overestimate as a safety precaution.

Pressure Profile

Similar to the temperature profile, we also needed to create a pressure profile for the duration of the rocket's flight. To do this, we used HyperCFD to determine the pressure on the tip of the nose cone and the body region of the nose cone. These pressures vary significantly since the tip experiences the brunt of the force during flight. We calculated the pressure of each region for the duration of the flight, which was dependent on Mach number and altitude. The differential pressure on the sides of the nose cone never exceeds 1atm, so everything except the tip pressure can be neglected.

Materials Modeling and Results

The primary simulation method used was finite element analysis using COMSOL Multiphysics. Time-dependent simulations using the *Heat Transfer in Solids* module were created to determine how deep the degradation temperature isotherm reached throughout the flight. Stationary simulations use the *Solid Mechanics* module to ensure that the coatings can survive the theoretical maximum aerodynamic forces.

The object in Figure 6 is an axially symmetric component with geometry based on the USC Traveler IV nose cone, extracted using imageJ. There are three domains: a base of coating material, an Inconel 718 spherical tip, and an Inconel 718 tip base.

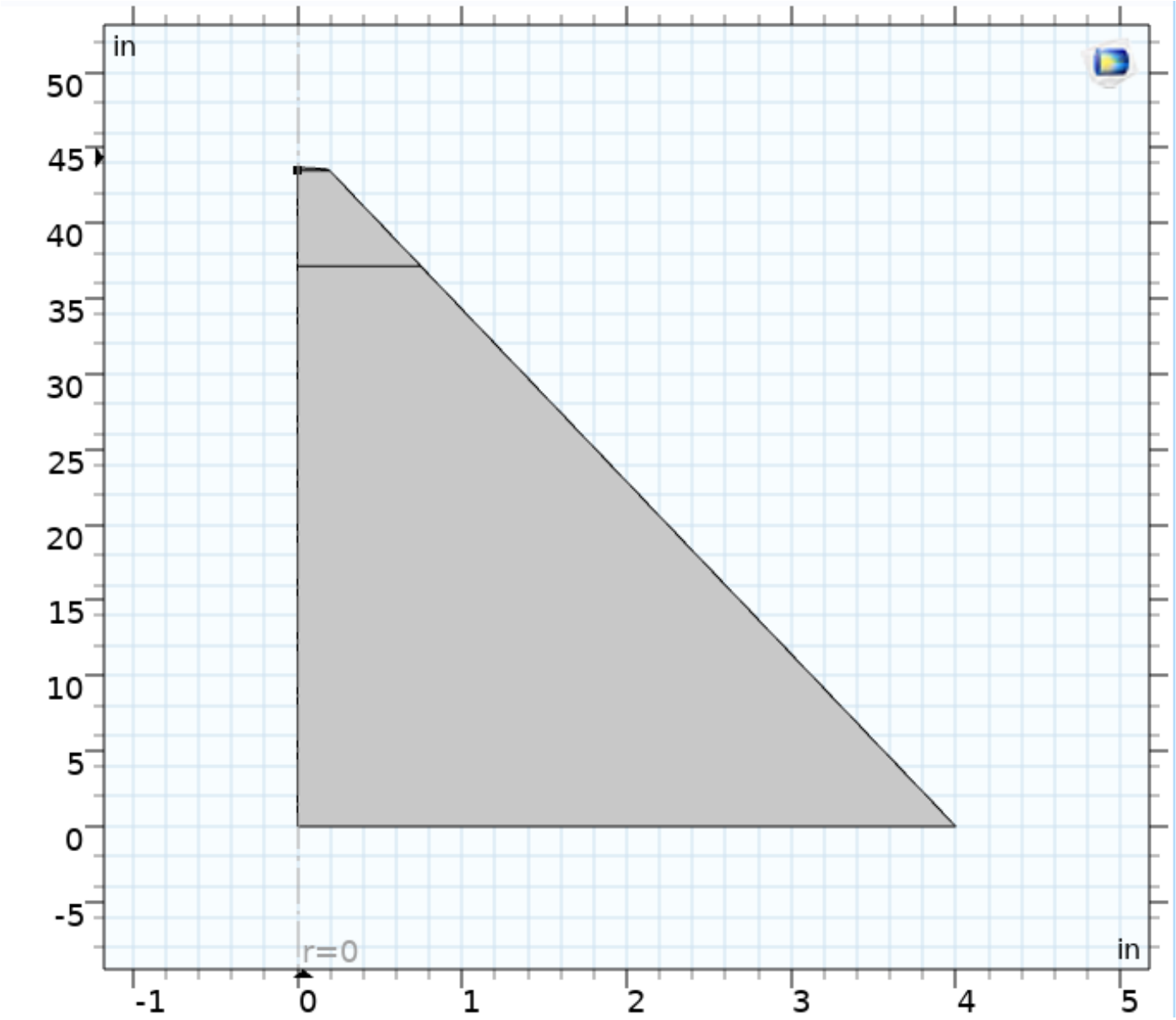

Figure 6: Thermal model geometry with vertical compression

For the temperature simulations, the left and bottom edges were given symmetry conditions. The temperature profile was applied as a boundary condition for the surface of the nose cone. Given the temperature over time, we viewed the maximum depths penetrated by the 275 °C limit boundary for different materials.

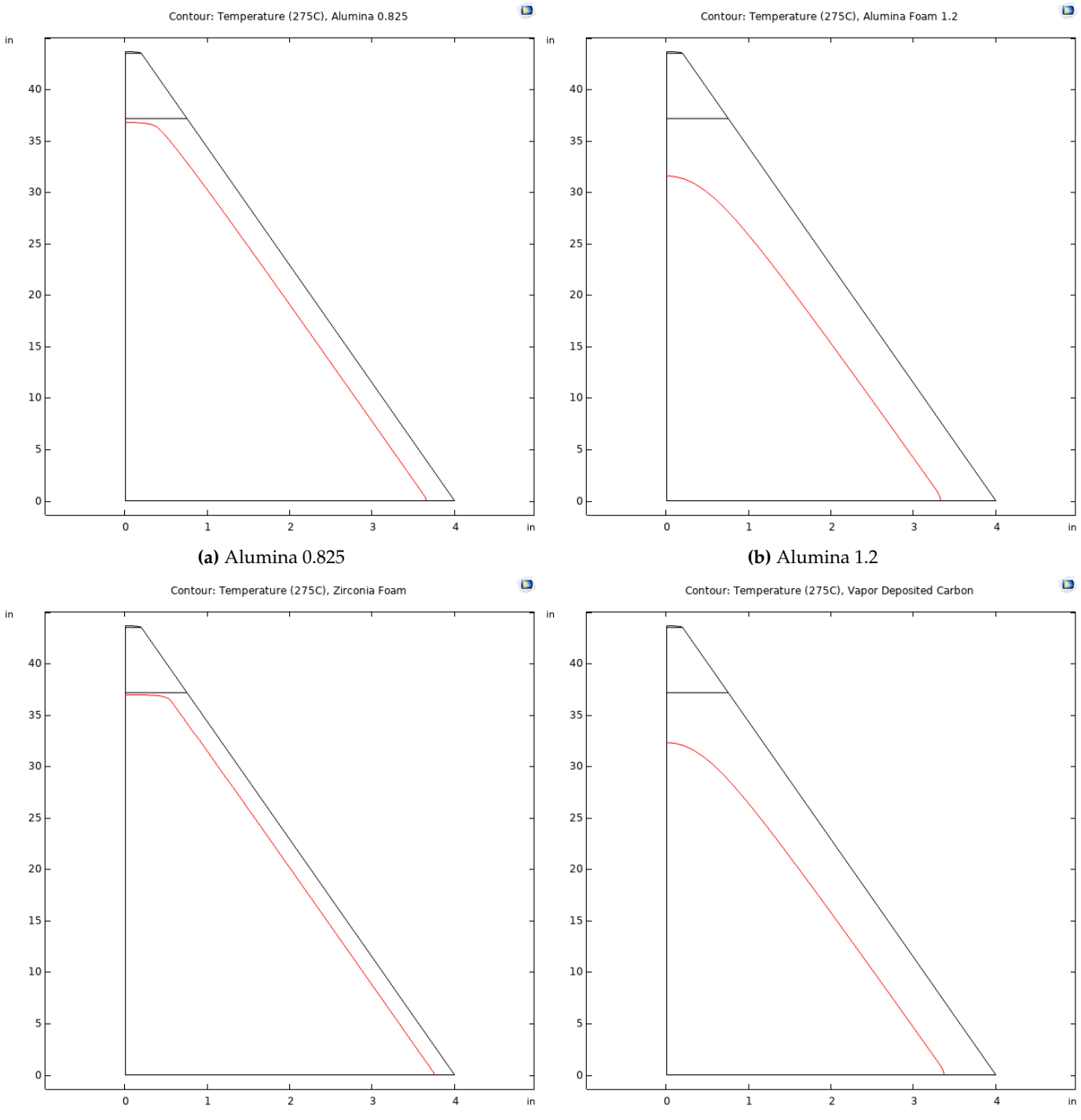

(a) Alumina 0.825

(b) Alumina 1.2

(c) Zirconia 1.23

(d) Vapor Deposited Carbon

Figure 7: Maximum-depth isotherms for different barrier materials

Based on the depths reached, vapor deposited carbon was eliminated as the thickness needed for sufficient protection would be impossible to produce, and $1.2\frac{g}{cm^3}$ alumina foam was eliminated due to being too thick to reasonably use. Given the thicknesses of 0.25" and 0.33" needed for the zirconia and alumina foams, the weights of insulation made from each material would be 5.83lbs and 5.12lbs respectively, so the difference is not as significant as the densities would suggest. We also tested the maximum forces that would be experienced during flight if the full load was somehow transferred to the foam. Using the USC data and the atmospheric pressures, we found the maximum pressure on the tip of the nose cone during flight using Hy-

perCFD [14] and set that as a solid mechanics edge condition. The models were reshaped to shells with thicknesses equal to the maximum penetration depths found, and the von Mises stress distributions (seen in Figure 8) were calculated.

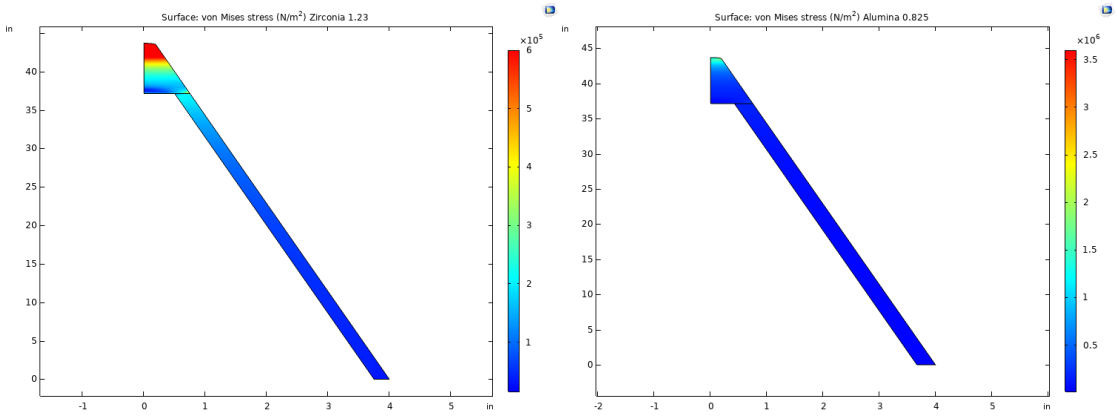

Figure 8: Maximum possible in-flight Stresses

For both plots, the color bar is adjusted so that stresses at or above the insulation material's yield strength are colored red. Since the only red regions are in the Inconel tip, we can safely assert that bulk yielding will not occur with either foam material even with a catastrophic delamination event.

Final Materials Selection

Given that both 0.825 alumina foam and 1.23 zirconia foam are viable candidates for use in our nose cone, we compared a few different properties to make the final decision. We first performed a thorough investigation of phase transformations to ensure none would occur within the predicted range of temperatures experienced during flight. Alumina, once transformed into the α phase, is thermodynamically stable and will not undergo any phase transformations in the range of temperatures experienced during flight [15]. Zirconia, on the other hand, would typically undergo a tetragonal to monoclinic phase transformation at 1170 °C, which leads to a 3-5% increase in volume. This phase transformation can be suppressed by adding MgO. Thus, the zirconia foam we considered for use contains 3.5% MgO, which stabilizes the zirconia at high temperatures. The high fracture toughness and strength displayed by zirconia is a result of controlling the volume expansion due to the phase transformation [16]. After guaranteeing phase stability of both cadidate materials, we compared a few different properties. Weight and the coefficient of thermal expansion are both important properties to minimize, however, they were reasonably similar for both materials so a decision was not made based on either. The material used needs to be radio frequency transparent, which both were [17]. We finally chose fracture toughness as the deciding property. We anticipate there will be mistakes made during the sol-gel manufacturing process, since this is a technique new to NUSTARS. Very small pores accidentally formed may be prone to inducing fracture, and general construction and handling of the rocket may subsequently introduce fracture conditions. In this case, we would like our nose cone to be resistant to crack propagation, hence, the choice of high fracture toughness. Based on this rationale, zirconia will be used for both the foam layer and the painted layer overlaying the foam.

Final Materials Design

The design specifications of our material are detailed in this section. The first element of our design is the dual-layer coating. The outer layer is a smooth, painted coat of zirconia, while the inner layer is thick, insulating zirconia foam. Using a two-layer design allows us to optimize the nose cone for multiple performance

criteria that would be difficult to meet using a single layer. The smooth outer coating reduces the drag coefficient, while the porous inner coating provides exceptional high temperature resistance. Using a foam also ensures the coating is relatively lightweight. By using the same base component (zirconia) for both layers, we also ensure mechanical stability and good adhesion between the two layers. The two layers will have the same thermal expansion behavior upon heating, thus eliminating mechanical failure that could occur from dissimilar volume changes. Another crucial design decision is the incorporation of MgO in the zirconia. This stabilizes the zirconia, and suppresses a phase transformation that would typically occur around our maximum anticipated temperature during flight. This phase transformation suppression increases mechanical stability by eliminating a significant volume change. The next few design specifications deal with the structure of the foam layer. We have elected to use open-cell foam in lieu of closed-cell foam. The structure of each foam can been seen in Figure 9 [18]. Open-cell foam is superior for high-temperature applications because of the high air content, and is also the lighter option [19]. We have chosen a density of 1.23 $\frac{g}{cm^3}$ for our zirconia foam because of the high fracture toughness it affords. Other densities (and thus, porosities) are possible, but they have lower fracture toughnesses, and thus we determined that this density best suits our needs. Finally, our foam will have a mesopore structure. Pore size does not greatly impact mechanical or thermal properties, however, extremely small pore sizes can be prone to fracture due to small radii of curvature [20]. To eliminate possible sources of failure, we will create mid-size pores during processing.

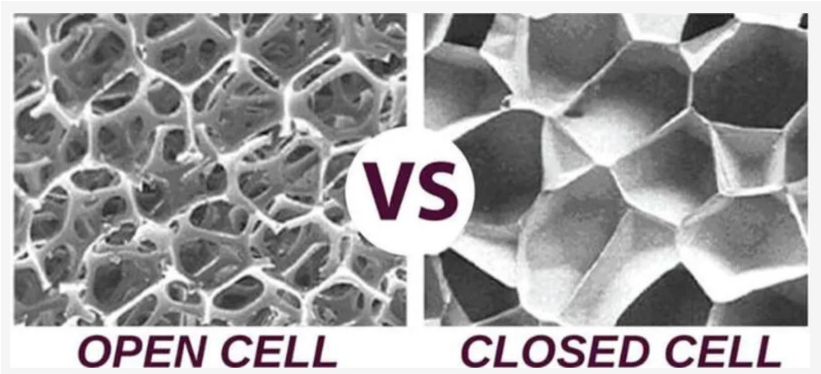

Figure 9: Cell comparison

Conclusion

In this report, we detail the process of selecting and designing a material for use in a nose cone thermal protection system on a space-capable rocket. The material must meet a rigorous set of standards and metrics; these were derived from our System Design Chart[2], which displays key processing-structure-property-performance relationships. Using these metrics, a GRANTA EduPack materials selection process narrowed the set of possible materials to four candidates. These materials were inputs to the computational stage of the project, which employed the use of the finite element software COMSOL Multiphysics and the computational fluid dynamics software HyperCFD. The modeling process further narrowed the options to magnesia-stabilized zirconia foam and low-density alumina foam, both with a solid painted surface of the same material. Comparing the two options, we selected zirconia foam as our final material. When contrasting the materials, the deciding factor was the higher fracture toughness of zirconia foam. The better performance permits a sol-gel manufacturing process which, while new to NUSTARS, is simple enough for students to use, and can be customized to adjust the structure of the material.

Future steps for this project would focus on determining optimal processing parameters such as colloidal pH, dry time, stabilizer concentration, mold design, and sintering.

References

[1] Benefits Stemming from Space Exploration (Sept 2013).
URL https://www.nasa.gov/sites/default/files/files/Benefits-Stemming-from-Space-Exploration-20 pdf

[2] COMSOL Multiphysics (2021).

[3] Traveler IV.
URL http://www.uscrpl.com/traveler-iv

[4] K. Ishizaki, S. Komarneni, M. Nanko, Sol-gel processing, designing porosity, pore size and polarity, and shaping processes, in: R. G. Ford (Ed.), Porous Materials, Vol. 4, Springer US, Boston, MA, 1998, pp. 67–180, series Title: Materials Technology Series. doi:10.1007/978-1-4615-5811-8_4.
URL http://link.springer.com/10.1007/978-1-4615-5811-8_4

[5] M. Higgins, Chemical vapor deposition benefits and limitations.

[6] C. C. Beozzo, M. A. Alves-Rosa, S. H. Pulcinelli, C. V. Santilli, Liquid Foam Templates Associated with the Sol-Gel Process for Production of Zirconia Ceramic Foams, Materials 6 (5) (2013) 1967–1979. doi:10.3390/ma6051967.

[7] S. Carstens, C. Splith, D. Enke, Sol-gel synthesis of α-Al 2 O 3 with enhanced porosity via dicarboxylic acid templating, Scientific Reports 9 (1) (2019) 19982. doi:10.1038/s41598-019-56294-1.

[8] CES EduPack Software, Granta Design Limited, Cambridge, UK (2009).

[9] G12-1.5.
URL https://wildmanrocketry.com/products/g12-1-5

[10] Isentropic Flow Equations.
URL https://www.grc.nasa.gov/www/BGH/isentrop.html

[11] A. Aitoumeziane, P. Eusebio, C. Hayes, V. Ramachandran, J. Smith, L. S. Regis, M. Stephenson, N. Tewksbury, M. Tran, H. Yang, Traveler IV Apogee Analysis 24.

[12] 1976 Standard Atmosphere Calculator.
URL https://www.digitaldutch.com/atmoscalc/

[13] W. M. Bland Jr., K. A. Collie, Free-flight aerodynamic-heating data to mach number 10.4 for a modified von karman nose shape, NASA Technical Note (D-889).

[14] John Cipolla, HyperCFD.
URL http://aerorocket.com/hyperx.html

[15] I. Levin, D. Brandon, Metastable Alumina Polymorphs: Crystal Structures and Transition Sequences, Journal of the American Ceramic Society 81 (8) (1998) 1995–2012, _eprint: https://ceramics.onlinelibrary.wiley.com/doi/pdf/10.1111/j.1151-2916.1998.tb02581.x. doi:10.1111/j.1151-2916.1998.tb02581.x.

[16] D. L. Porter, A. H. Heuer, Microstructural Development in MgO-Partially Stabilized Zirconia (Mg-PSZ), Journal of the American Ceramic Society 62 (5-6) (1979) 298–305, _eprint: https://ceramics.onlinelibrary.wiley.com/doi/pdf/10.1111/j.1151-2916.1979.tb09484.x. doi:10.1111/j.1151-2916.1979.tb09484.x.

[17] B. Roemmele, Apple has advanced the use of Aluminum to such a degree they have reached the pinnacle. (Sep. 2016).
URL https://medium.com/@brianroemmele/apple-has-advanced-the-use-of-aluminum-to-such-a-degree-

[18] Dissecting Open Cell Vs Closed Cell Foam - Second Skin Audio.
URL https://www.secondskinaudio.com/heat-insulation/open-cell-foam-vs-closed-cell-foam/

[19] Metal Foams – Properties, Production and Applications, section: Materials Article (Jan. 2013).
URL https://www.azom.com/article.aspx?ArticleID=8097

[20] W.-Y. Jang, S. Kyriakides, A. M. Kraynik, On the compressive strength of open-cell metal foams with Kelvin and random cell structures, International Journal of Solids and Structures 47 (21) (2010) 2872–2883. doi:10.1016/j.ijsolstr.2010.06.014.